

Polarization effects in a highly birefringent nonlinear photonic crystal fiber with two-zero dispersion wavelengths

Brendan J. Chick, James W.M. Chon and Min Gu

Centre for Micro-Photonics, Faculty of Engineering and Industrial Sciences, Swinburne University of Technology, P.O. Box 218, Hawthorn, 3122, Victoria, Australia.

mgu@swin.edu.au

Abstract: A theoretical and experimental study is presented on polarized pulsed propagation from a highly birefringent nonlinear photonic crystal fiber with two-zero dispersion wavelengths. Experimental observations show that the input polarization state can maintain its linearity and that the fiber birefringence creates different spectral properties dependent on the input polarization orientation. The most extensive spectra are obtained for a coupling polarization angles aligned with the fast and slow axis, which is created by the high-order dispersion and Kerr nonlinearity.

© 2008 Optical Society of America

OCIS codes: (190.4370) Nonlinear optics, fibers; (190.5530) Pulse propagation and temporal solitons; (260.543) Polarization;

References and links

1. J. K. Ranka, R. S. Windeler, and A. J. Stentz, "Visible continuum generation in air-silica microstructure optical fibers with anomalous dispersion at 800 nm," *Opt. Lett.* **25**, 25-27 (2000).
2. I. Hartl, X. D. Li, C. Chudoba, R. K. Ghanta, T. H. Ko, J. G. Fujimoto, J. K. Ranka, and R. S. Windeler, "Ultrahigh-resolution optical coherence tomography using continuum generation in an air-silica microstructure fiber," *Opt. Lett.* **26**, 608-610 (2001).
3. H. N. Paulsen, K. M. Hilligsøe, J. Thøgersen, S. R. Keiding, and J. J. Larsen, "Coherent anti-Stokes Raman scattering microscopy with a photonic crystal fiber based light source," *Opt. Lett.* **28**, 1123-1125 (2003).
4. Th. Udem, R. Holzwarth, and T. W. Hänsch, "Optical frequency metrology," *Nature* **416**, 233-237 (2002).
5. J. E. Morris, A. E. Carruthers, M. Mazilu, P. J. Reece, T. Cizmar, P. Fischer, and K. Dholakia, "Optical micro-manipulation using supercontinuum Laguerre Gaussian and Gaussian beams," *Opt. Express* **16**, 1011-10129 (2008).
6. T. A. Birks, J. C. Knight, and P. St. J. Russell, "Endlessly single mode photonic crystal fiber," *Opt. Lett.* **22**, 961-963 (1997).
7. T. A. Birks, D. Mogilevtsev, J. C. Knight, and P. St. J. Russell, "Dispersion compensation using single-material fibers," *IEEE Photon. Technol. Lett.*, **11**, 674-676, (1999).
8. W. H. Reeves, D. V. Skryabin, F. Biancalana, J. C. Knight, P. St. J. Russell, F.G.Omenetto, A. Efimov, and A. J. Taylor, "Transformation and control of ultrashort pulses in dispersion-engineered photonic crystal fibres," *Nature*, **474**, 511-515 (2003).
9. T. V. Andersen, K. M. Hilligsøe, C. K. Nielsen, J. Thøgersen, K. P. Hansen, S. R. Keiding, and J. J. Larsen, "Continuous-wave wavelength conversion in a photonics crystal fiber with two zero-dispersion wavelengths," *Opt. Express* **12**, 4113-4122 (2004).
10. Z. Zhu and T. G. Brown, "Polarization properties of supercontinuum spectra generated in birefringent photonic crystal fibers," *J. Opt. Soc. Am. B*, **21**, 248-257, 2004.
11. Z. Zhu and T. G. Brown, "Experimental studies of polarization properties of supercontinua generated in a birefringent photonic crystal fiber," *Opt. Express* **12**, 791-796 (2004).
12. R. H. Stolen and C. Lin, "Self-phase-modulation in silica optical fibers," *Phys. Rev. A*, **17**, 1448-1453 (1978).

13. M. Miyagi and S. Nishida, "Pulse spreading in a single-mode fiber due to third-order dispersion," *Appl. Opt.* **18**, 678–682 (1979).
14. G. P. Agrawal, "Nonlinear fiber optics," 3rd ed. (Academic San Diego, Calif., 2002).
15. S. Coen, A. H. L. Chau, R. Leohardt, J. D. Harvey, J. C. Knight, W. J. Wadsworth, and P. St. J. Russell, "Supercontinuum generation by stimulated Raman scattering and parametric four-wave mixing in photonic crystal fibers," *J. Opt. Soc. Am. B* **19**, 753–764 (2002).
16. I. Cristiani, R. Tediosi, L. Tartara, and V. Degiorgio, "Dispersive wave generation by solitons in microstructured optical fibres," *Opt. Express* **12**, 124–135 (2004).
17. M. J. Steel, T. White, C. Martijn de Sterke, R. C. McPhedran, and L. C. Botten, "Symmetry and degeneracy in microstructured optical fibers," *Opt. Lett.* **26**, 448 (2001).
18. N. Karasawa, S. Nakamura, N. Nakagawa, M. Shibata, R. Morita, H. Shigekawa, and M. Yamashita, 2001, "Comparison between theory and experiment of nonlinear propagation for a-few-cycle and ultra broadband optical pulses in a fused-silica fiber," *IEEE J. Quant. Electron.* **37**, 398–404 (2001).
19. K.J. Blow and D. Wood, "Theoretical description of transient stimulated Raman scattering in optical fibers," *IEEE J. Quant. Electron.* **25**, 2665–2673 (1989).
20. J. Herrmann, U. Griebner, N. Zhavoronkov, A. Husakou, D. Nickel, J. C. Knight, W. J. Wadsworth, P. St. J. Russell, and G. Korn, "Experimental evidence for supercontinuum generation by fission of higher-order solitons in photonic fibers," *Phys. Rev. Lett.*, **88**, 173901 (2002).
21. J. M. Dudley, G. Genty, and S. Coen, "Supercontinuum generation in photonic crystal fiber," *Mod. Phys. Rev.*, **78**, 113–1184 (2006).

1. Introduction

Supercontinuum (SC) generation in nonlinear photonic crystal fibers (PCFs) due to the generation of their small core [1] has been pursued in many areas such as optical coherence tomography (OCT) [2], coherent anti-Stokes Raman scattering microscopy (CARS) [3], optical metrology [4] and optical trapping [5]. SC generation caused by engineered dispersion and nonlinearity can be easily demonstrated with high power continuous wave lasers or pulsed laser systems.

Three structural properties of PCFs allow the modification of dispersion and nonlinearity; the air-fill fraction; a one-dimensional asymmetry; and the core size. Dispersion engineering by the manipulation of the air hole structure of a PCF [6, 7, 8], allows the guidance of the optical wave to be influenced by different dispersion effects. By using a low hole diameter to pitch ratio (0.6) and maintaining a small core diameter ($1.8\ \mu\text{m}$) the second order dispersion profile can be tailored to have two-zero dispersion wavelengths (ZDWs) which is known to enhance nonlinear processes such as four-wave mixing [9] and higher-order dispersion effects.

A one-dimensional asymmetry (e.g. the increase of two holes either side of the core) will cause different propagation parameters for the fundamental linearly polarized modes, creating birefringence. The incorporation of high birefringence, dispersion and nonlinearity allows the maintaining of the coupled polarization state while generating a SC [10, 11]. Highly polarized coherent white light could be of use in microscopy and optical pump probe systems.

The core size affects the pulse propagation by the introduction of nonlinearity and is inversely proportional to the effective modal area. Nonlinearity induced by the Kerr effect causes the spectral splitting and the sum frequency generation in PCFs [12]. The dominant nonlinear effect in PCFs is self phase modulation, where the effective refractive index is modulated by the intensity causing the group velocity to fall. Due to the high peak intensity of femtosecond pulses, nonlinearity induced by self phase modulation can easily be achieved.

The extent of SC generation is enhanced in the anomalous dispersion regime, where the carrier frequency of the coupled light is close to the ZDW. In this region four-wave mixing is the strongest causing strong Stokes and Anti-Stokes frequencies [9]. In the femtosecond regime the third-order dispersion is the dominant broadening mechanism and a high degree of curvature in dispersion is required to enhance the third-order term [13]. Since the geometry of fibres with two ZDWs inherent these characteristics, they are of particular interest in generating extensive SC spectra.

To date, what has not been shown is an experimental and theoretical study of polarized pulse propagation of femtosecond pulses in two ZDWs nonlinear photonic crystal fiber. This study uses current theoretical methodology to understand the principles of polarized light propagation under the influence of two ZDWs. An explanation is given for why the spectra are different for different input polarisation orientations. A comparison is made between the theoretical and experimental degree of polarization.

2. Numerical study

The polarization evolution in nonlinear PCF is modelled using the coupled mode nonlinear Schrödinger equation (CMNLSE) [14, 15], given by:

$$\frac{\partial A_j}{\partial z} + \frac{1}{2} \left(\Delta\beta_0 + \Delta\beta_1 \frac{\partial A_j}{\partial t} \right) - \sum_{m \geq 2} \frac{i^{m+1}}{m!} \beta_{mj} \frac{\partial^m A_j}{\partial t^m} = i\gamma \left(1 + i\tau_0 \frac{\partial}{\partial t} \right) A_j \left((1 - f_R) \left[|A_j|^2 + \frac{2}{3} |A_k|^2 \right] + f_R R_j(z, t) \right) \quad (1)$$

$$R_j(z, t) = \int_{-\infty}^t h_R(t - t') \left(|A_j|^2 + |A_k|^2 \right) dt' \quad (2)$$

where A_j and A_k are the field components with j and $k = x$ or y ($x \neq y$), z is a propagation coordinate, the time coordinate moving in a reference frame is given by $t = \tau - (\beta_{1j} + \beta_{1k})z/2$, β_m is the m^{th} order propagation coefficient, $\Delta\beta_0 = (\beta_{0j} - \beta_{0k})$ is the phase mismatch, $\Delta\beta_1 = (\beta_{1j} - \beta_{1k})$ is the group velocity mismatch, γ and τ_0 are the nonlinearity and optical shock coefficients respectively. The simulation method used in this study is the symmetrized split-step Fourier method [14] utilising a fourth order Runge Kutta method for the nonlinear integration [16].

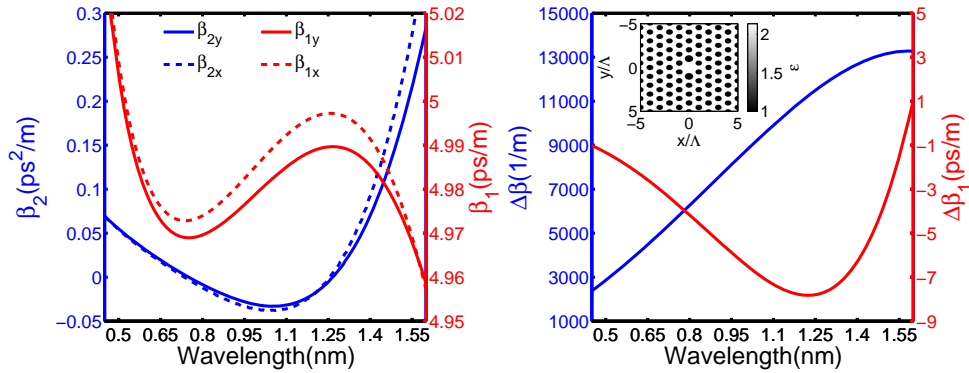


Fig. 1. The dispersion coefficients related to the mode propagation constant β . The left hand side of the figure shows the first- and second-order dispersion coefficients for the two fundamental modes. The right hand side shows the phase mismatch ($\Delta\beta_0$) and the group velocity mismatch ($\Delta\beta_1$) between these modes. The inset is the crystal geometry in relation to the presented curves.

The propagation constant, for the two fundamental propagating modes were calculated using plane wave theory [17] This data set is expanded into a Taylor series to obtain the dispersion coefficients (Eq. (3)) and phase mismatch (Eq. (4)) which is used to find $\Delta\beta_0$ and $\Delta\beta_1$. The

mode profiles as a function of frequency can be used to calculate the nonlinear terms γ and τ_0 [18, 19].

$$\beta_j(\omega) = \beta_{0j} + \beta_{1j}(\omega - \omega_0) + \frac{\beta_{2j}}{2!}(\omega - \omega_0)^2 + \frac{\beta_{3j}}{3!}(\omega - \omega_0)^3 \dots \quad (3)$$

$$\Delta\beta_j(\omega) = \Delta\beta_{0j} + \Delta\beta_{1j}(\omega - \omega_0) + \frac{\Delta\beta_{2j}}{2!}(\omega - \omega_0)^2 + \frac{\Delta\beta_{3j}}{3!}(\omega - \omega_0)^3 \dots \quad (4)$$

Table 1. Dispersion data for the polarized mode of the nonlinear fibre.

β_m	mode y(ps^m/m)	mode x(ps^m/m)
β_2	$-4.654e^{-3}$	$-8.215e^{-3}$
β_3	$4.879e^{-5}$	$5.063e^{-5}$
β_4	$-1.735e^{-8}$	$-2.118e^{-8}$
β_5	$1.42e^{-10}$	$2.018e^{-10}$
β_6	$1.802e^{-13}$	$1.356e^{-13}$
β_7	$-6.964e^{-15}$	$-8.764e^{-15}$
β_8	$3.095e^{-17}$	$3.979e^{-17}$
β_9	$-4.649e^{-20}$	$-6.02e^{-20}$

Figure 1 shows the first- and second-order dispersion terms. Both curves are different due to fiber birefringence and the consequence is that the two modes have different ZDWs. The difference between the two polarized modes is significant and conveys the importance of the group velocity mismatch. The inset of Fig. 1 shows the geometry of the fiber structure where the fundamental modes are aligned with the x and y axes. The first-order dispersion term is related to the group velocity by the relation, $\beta_1 = 1/v_g$. The data in Fig. 1 show that the y-polarized mode travels faster than the x-polarized mode and called the fast axis and slow axes, respectively. The dispersion properties used in this study are shown in table 1. The changes in optical nonlinearity and optical shock are insignificant between modes and for this study are 0.095 W/m and 0.57 fs, respectively. The phase mismatch and group velocity mismatch are $\pm 61201/m$ and $\pm 3.984ps/m$, respectively.

Equation 1 was used to calculate 87 fs pulses propagating at different input polarization orientations. A pulse width of 87 fs and a fiber length of 130 mm were chosen to coincide with experimental conditions.

Figure 2 shows the output spectra obtain from a nonlinear PCF pumped with 87 fs pulses at input polarization orientations of 0 (y-axis), 45 and 90 (x-axis) degrees. The simulation shows that the polarization state is maintained for light coupled into either the x-polarized or y-polarized axis of the fiber. The x-polarized mode has the most extensive spectra and this is because the pump wavelength undergoes a stronger initial compression caused by the stronger second-order dispersion term. For input polarisation orientation of 45 degrees, the degree of polarization is not maintained due to an equal coupling between modes and the spectra are different due to the relative strength of the second- order dispersion.

When the pulse enters the nonlinear fibre, it undergoes a transformation to form a high-order soliton. The high-order soliton then breaks up in a fission process which converts it into lower-order solitons [20]. The order of the initial soliton and the length at which soliton fission occurs is given by [21]:

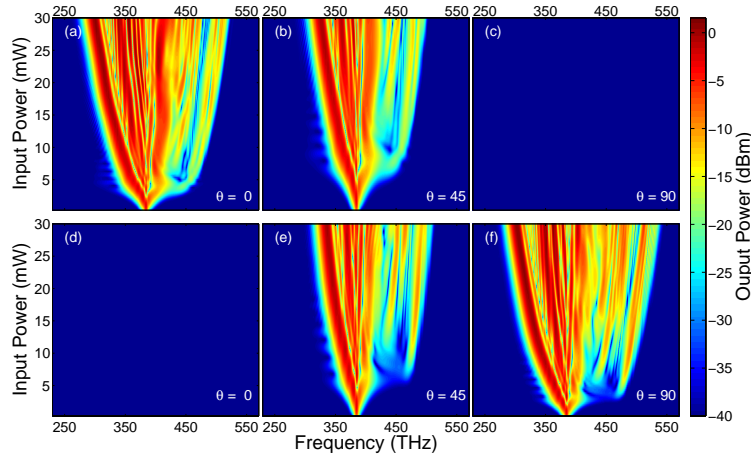


Fig. 2. Theoretically obtained spectra of propagation within a 130mm NL-PCF with a 87fs pulse. Figures (a), (b) and (c) are the spectra for the y polarized output field with (d), (e) and (f) for the x polarized output field. θ is the input polarization angle with respect to the y axis.

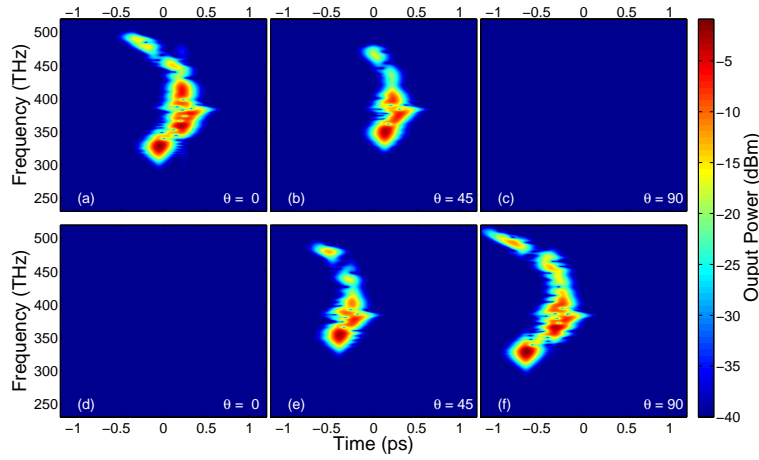


Fig. 3. Theoretically obtained spectral and temporal profile of 87fs pulsed propagation within a 130mm nonlinear PCF. Figures (a), (b) and (c) are the spectra for the y polarized output field with (d), (e) and (f) for the x polarized output field.

$$N = \left(\frac{\gamma P_0 T_0^2}{|\beta_2|} \right)^{1/2} \quad (5)$$

$$L_f = \frac{T_0^2}{|\beta_2|} \frac{1}{N} \quad (6)$$

where P_0 is the peak power and T_0 is the full width at half maximum.

Although the soliton order is higher along the y axis in comparison to the x axis, the fission

length is 0.0465 m and 0.035 m, respectively, which could be attributing to the more extensive spectra. Although there are some differences between the spectral components between input polarization orientations, the spectra are similar and hence both axes could be used for polarized broadband applications.

Figure 3 confirms that the output spectra are different between the two fundamental modes. The output spectra for the y-polarized mode travels at a higher speed compared to the x-polarized mode which is due to the group velocity mismatch. Fig. 3 (a) and (f) show the difference in the pulse structure and is due to the different dispersion properties and fission processes of the coupled axes. The effects observed would be important to consider in time-resolved polarized illumination applications since there is a delay between spectral features.

3. Experimental study

The experimental setup is shown in Fig. 4. A pulsed light beam from a Ti:Sapphire laser was coupled into a nonlinear PCF (Crystal-fibre). Two Glan Thomson polarizers were used to vary the input power and a half wave plate to alter the input polarisation orientation. The output pulse was analyzed with a Glan Thomson polarizer. Spectra were observed and recorded using an Ando spectrometer and Princeton Instruments CCD (pixis 100). The pulsed propagation spectra were obtained for different input polarization orientations. The characteristics of the fiber used in this experimental study are shown in Fig. 1 and table 1.

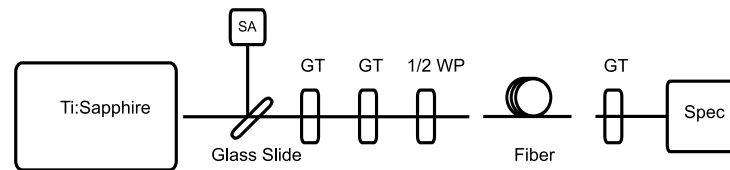


Fig. 4. Optical arrangement used in this study. GT - Glan Thomson, WP - Wave Plate, Spec - Spectrograph and SA - Spectrum Analyser

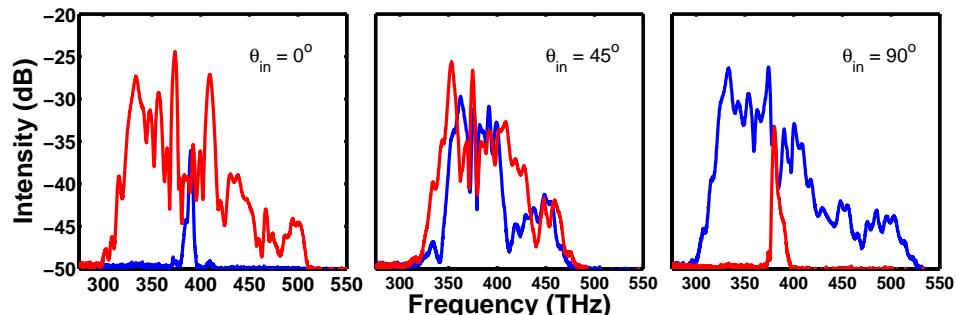


Fig. 5. Spectral properties of the polarized modes of the nonlinear PCF. The perpendicular (blue) and parallel polarized (red) states are with reference to the output orientation of the laser.

Figure 5 shows the spectra for the two output modes of the PCF coupled with 780 nm, 87 fs pulses and 15 mW average power. The spectra show the high degree of polarization for the input

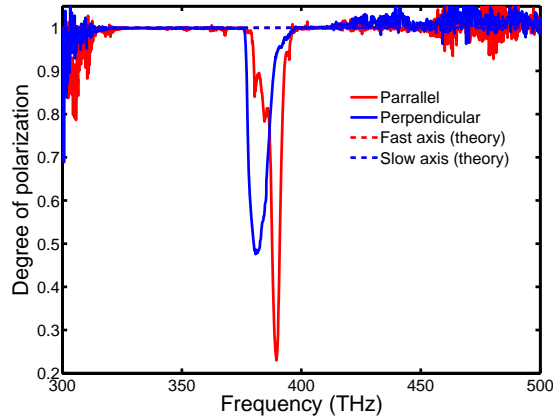


Fig. 6. Degree of polarization for the fast and the slow axes of the fiber.

pulse orientations of 0 and 90 degrees. In addition, a large degree of the red-shifted radiation attributed to stimulated Raman scattering is present. The 0 and 90 degree spectra are different and confirm the theoretically obtained results. For 0 degrees it is apparent that there is a blue-shift of radiation and is attributed to the dispersive wave generation and four-wave mixing. In addition, a small amount of radiation is coupled into the orthogonal mode which is attributed to the depolarization by the high numerical aperture input coupling.

The degree of polarization (DOP), defined as $DOP = (I_{||} - I_{\perp}) / (I_{||} + I_{\perp})$, is shown in Fig. 6. The experimental curves show a strong degree of polarization for all wavelengths except for the pump bandwidth. This confirms the high degree of polarization measured in Fig. 5. The theoretical degree of polarization shows the effects of depolarization are not attributed to cross coupling and must be introduced by the input coupling.

4. Conclusion

A highly birefringent PCF with two ZDWs is beneficial to produce extensive highly-polarized optical spectra due to the nonlinear and dispersive properties inherited from its geometry. A methodology for generating broadband pulsed light from a two ZDWs PCF is presented. The theoretical and experimental observation shows that the spectra maintain its linear polarization state and that the extent of the spectra is stronger at either of the fundamental mode axes. By pumping the fiber at one of the modal ZDWs, four-wave mixing can be amplified and form strong anti-Stokes radiation in the visible region.